# Suggestion and Modeling of a Novel Capsular Microrobot with Surface Forces

R. Nadafi D. B., M. Kabganian
*R. Nadafi (Msc. Student, Faculty of Mechanical Engineering, Amirkabir University, Iran),*
*M. Kabganian (Associate Professor, Faculty of Mechanical Engineering, Amirkabir University, Iran),*
*(Tel : 98-21-6454-3456; Fax :98-21 6641-9728)*
*(rezanadafi@gmail.com)*
*(kabgan@aut.ac.ir)*

***Abstract***: For development of endoscopic Capsular, a design of legged capsular microrobot whit polymeric actuators is suggested in this paper. First locomotion of microrobot is explained then microrobot is modeled by envisage exerting surface forces and microactuator. Surface forces contain slip-friction, surface adhesion and resting adhesion and polymeric microactuators is ionic polymer metal composite. Time variant response of polymeric microactuators is modeled fundamental of coupled electromechanical equations and electric equivalent bulk gel polymeric.

Results simulation of dynamical model microrobot shows that best installation angle of legs is 60 degree, proper mass of microrobot is 2g and speed marching is 1 millimeter per second.

***Keywords***: Microrobot, Endoscopy, Microactuator, Ionic Polymer Metal Composite, Resting Adhesion, Surface Adhesion, Modul.

## I. INTRODUCTION

Passive capsular endoscopy has born since 2001. Because of painful of endoscopy, researchers offered capsulated device endoscope. Noncontrolability, slow motion and etc. had to MEMS researchers attention subject of capsular microrobotics. Microrobots are offered with usual microactuators for example SMA, IPMC, micromotor, piezoelectrics and etc [1]-[4]. Suitable device for specific applications is not offered so far.

This device of proposed capsular microrobot that having 8 polymeric legs, is lifeagreeable. It needs 1volt and below 0.1 A For 1 mm/sec speed. Dynamic model of microrobot has derived to considering of surface forces and actuator model. Microrobot model is simulated to determine important parameters. This parameters are mass, installation angle of foots, stiffness of material between middle plates, amount of equivalent resistant and condenser of actuator, level of voltage and etc.

## II. Introduce of structure and walking mechanism of microrobot

This propounded microrobot has tow parts active and passive. Cylindrical active part of microrobot with 15mm length and 4mm diameter (Figure 1) products driving force. Cylindrical passive part of microrobot with 15mm length and 8mm diameter carries equipments. Active part have 8 symmetric legs (Figure2). Legs connects to body by rigid middle plates. Planar motion of microrobot is coming from polymeric legs. Figure 3 show how capsular microrobot forwards.

## III. Modeling Surface forces

### 1. Surface Adhesion

First time satto introduced method to used adhesion force for lift objects [9]. Surface Adhesion is contained of capillary, $F^c$ ,electrostatic, $F^e$ and vanderwaals, $F^{vdw}$ forces [9-13]. Figure4 show contrasting theses forces for tow contacted surfaces. Therefore $F^{Adh}$ is defined as equation (1).

*A. Capillary force*

Capillary forces, $F^c$: they are a manifestation of the surface tension of trapped capillary liquids that exert a force due to the Laplace pressure difference between the outside and inside of liquid junctions. Capillary forces is given by equation (2). for semispherical plate [8] , [9].

*B. Electrostatic force*

• Electrostatic forces, $F^e$: they can arise due to (a) an externally applied voltage across the interface; (b) difference in material work functions of the surfaces; (c) an electrostatic charging resulting from the release etc. Because legs of microrobot is fixed when walking then Electrostatic force of microrobot is considered zero.

*C. Vander waals Force*

Vander waals force to be calculated based on the interaction between individual atoms making up the particles. The non-retarded energy of interaction between two particles, 1 and 2, of volumes V1 and V2 containing q1 and q2 atoms per cm3 is defined by equation (3) [9]. The Vander waals force will be given by variation energy ( equation (3) ) directed to atomic distance that equation (4) has been solved for the vander Waals force equations between Spherical and plated surfaces [9]. Finally surface adhesion is determined at equation (5). L is external load and ..e is calculated by equation (6). S is shear strength of contacted plates and $P_e$ has introduced in [7].

## III. Modeling Ionic Polymer Metal Composite

Ionic polymer-metal composite (IPMC) which is an electroactive polymer that bends in response to electric stimuli. In this paper when input voltage is applied to it, cation ion which move freely in membrane is drawn to electrode by electric field with water molecule. Then one side of electrodes is dilated, and another shrank, thus IPMC membrane bends.

Kim (2003) has introduced mathematics IPMC model for direct task. relation between voltage (input ) and torque (output) is expressed in [1]:

## IV. Modeling Microrobot Motion

Dynamical microrobot model is determined basis of surface forces model, polymeric actuator model and proposed structure of microrobot. Figure (5) is free body diagram for each leg and its middle plate. $R_x$ is slip friction of passive part as load. F is reaction of wall. T and $K_y$ are IPMC torque and spring force respectively. equation (7) can write For Base point of Fig (5). I is inertia moment, l is leg length, K is spring stiffness and x is amount of motion. $R_x$ ( slip friction ) is defined basis of stribec friction [14]. T that torque of each IPMC leg is determined basis of equations (9) , (10). w is width of IPMC leg.

## V. UNITS

Use SI units unless is told.

## VI. FIGURES/TABLES

### 1. Figures

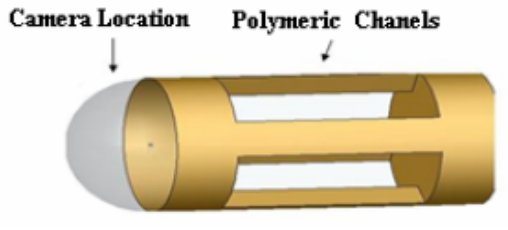


Fig.1. showing active part

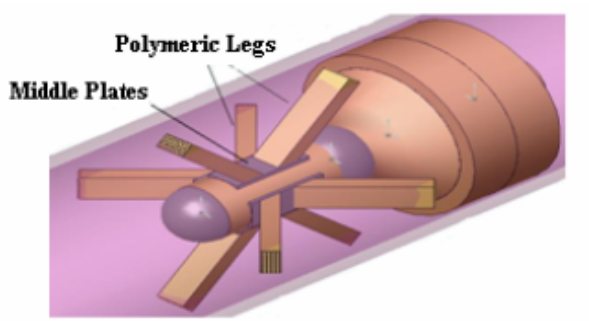


Fig.2. showing tow parts, Middle plates and Legs

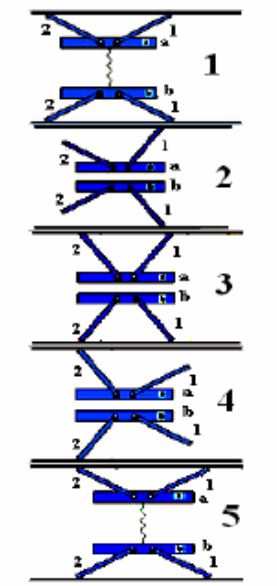


Fig.3. Waking principle and sequence of the ciliary motion based 8-legged walking device

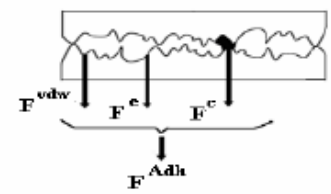


Fig.4. Component of surface adhesion [13]

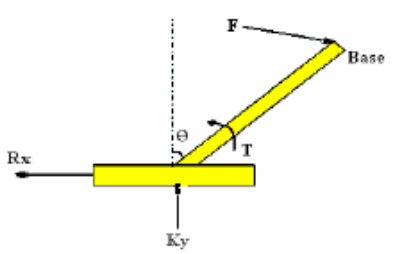


Fig 5. Free Body Diagram for leg and middle plate

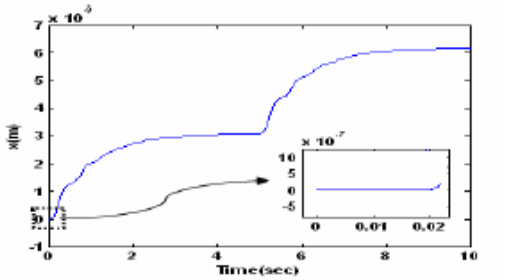


Fig 6. Motion diagram for center of mass Microrbot

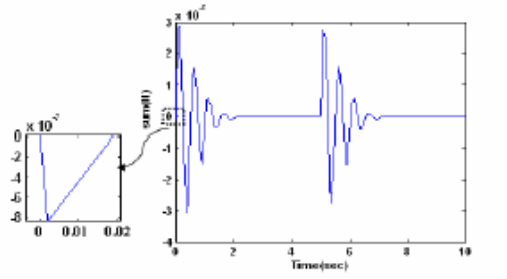


Fig 7. Time variant of resultant forces

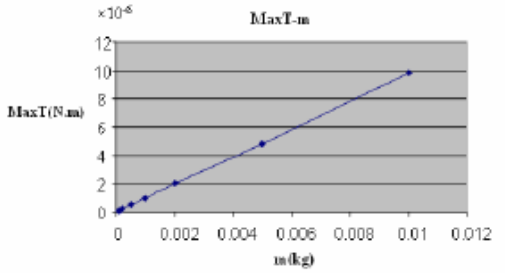


Fig 8. Effect of mass for maximum produced torque

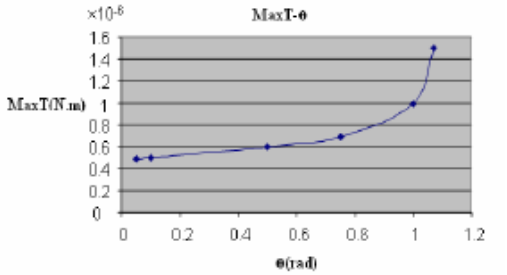


Fig 9. Effect of installed angle for maximum produced torque

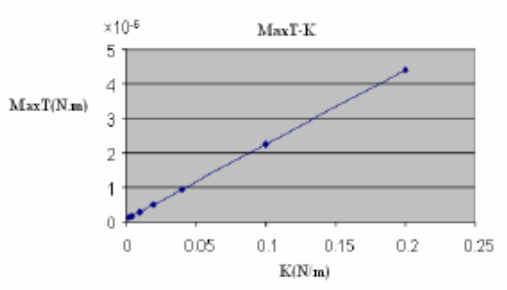


Fig 10. Effect of stiffness spring for maximum produced torque

## 2. Tables

Table 1. Numerical parameters of each IPMC leg [6]

| Parameter | $\sigma_0$ | $K_1$ | h(μm) | $L_1$ |
|---|---|---|---|---|
| Amount | 0.4 | $3.4\times10^{-17}$ | 200 | $10^{-8}$ |
| Parameter | $R_1$ | $R_2$ | C(F) | $V_A$(v) |
| Amount | 0.5 | 15 | 0.25 | 1 |

Table 2. Numerical parameters of slip friction[13]

| Parameter | $V_s$ | $F_s$ | $F_c$ | $F_v$ |
|---|---|---|---|---|
| Amount | 0.001 | 0.00015 | 0.0001 | 0.02 |

Table 3. Numerical parameters of surface forces[7]

| Parameter | $\eta(m^{-2})$ | R(μm) | $\Delta\gamma$ (J.m$^{-2}$) |
|---|---|---|---|
| Amount | $4\times10^{12}$ | 0.4 | 0.1 |
| Parameter | σ(μm) | $D(P_a^{-1})$ | $A_a(\mu m^2)$ |
| Amount | 0.04 | $9.1\times10^{-12}$ | 100 |

Table 4. Numerical parameters of robot Structure

| Para. | w (mm) | L (mm) | m (gr) | K (N/m) | θ (Deg) |
|---|---|---|---|---|---|
| Am. | 1 | 4 | 1 | 0.02 | 60 |

## 3. Equations

$$F^{Adh} = F^{e} + F^{c} + F^{vdw} \quad (1)$$

$$F^{c} = \frac{4\pi R_{ball}\gamma_l}{1+D_1} \quad (2)$$

$$E = -\int_{V_1} dV_1 \int_{V_2} dV_2 \frac{q_1 q_2 \lambda_{12}}{H^6} \quad (3)$$

$$F^{vdw} = \frac{AR}{6D^2} \quad (4)$$

$$F_f = \mu_e \left(F^{Adh} + L\right) \quad (5)$$

$$\mu_e = s/P_e \quad (6)$$

$$I\ddot{x} = T - \frac{1}{4} l\cos(\theta) R_x - Kl\sin(\theta)\tan(\theta)\, x \quad (7)$$

$$R_x = F_c + (F_s - F_c) e^{-\left(\frac{\dot{x}}{v_s}\right)^2} + F_v \dot{x} \quad (8)$$

$$T = \Gamma \times w \quad (9)$$

$$T = \frac{w}{12} \bullet \frac{1-2\sigma_p}{1-\sigma_p} \bullet \frac{L_I h^3}{K_I} \bullet \frac{0.5V_A}{h} \bullet \left\{ 1 - \frac{R_2}{R_2+2R_1} - \frac{2R_1.R_2}{R_2(R_2+2R_1)} \bullet \right\} \bullet \left\{ \bullet \exp\left( -\left( \frac{R_2+2R_1}{R_1.R_2.C} \right).t \right) \right\} \quad (10)$$

## VII. Conclusion of Open Loop Microrobot Simulation

Numerical parameter is considered basis of tables (1) – (4). Figures (6) and (7) show under 0.02 second the microrobot is stopped because resultant forces is negative (fig (7)).

1. If mass of microrobot beyond of 2gr then polymeric actuators is saturated (Fig (8)).
2. If installed angle beyond of 70 degree then polymeric actuators is saturated (Fig (9)) and IPMC legs can not driven force.
3. If stiffness spring of between middle plates beyond of 0.17 then polymeric actuators is saturated (Fig (10)) and IPMC can not motion middle plates.

## REFERENCES

[1] Byungkyu K., Sunghak L., Jong H., Design and Fabrication of a Locomotive Mechanism for Capsule-Type Endoscopes Using Shape Memory Alloys SMAs, IEEE/ASME TRANSACTIONS ON MECHATRONICS, VOL. 10, NO. 1, FEBRUARY 2005.

[2] Dario P, Menciassi A, et al., Modeling and Experiments on a Legged Microrobot Locomoting in a Tubular, Compliant and Slippery Environment, The International Journal of Robotics Research, Vol. 25, No. 5–6, May–June 2006.

[3] Dario P, Menciassi A, et al. Teleoperated endoscopic capsule equipped with active Locomotion system, Patent No. WO 2005082248. [2] Tsuchiya K (1995), Model dynamics and function of a complex system (in Japanese). Control inf 39(1):29-34

[4] Zvi Fireman, D Paz, Y Kopelman, Capsule endoscopy: Improving transit time and Image view, World Journal of Gastroenterology, 2005;11(37):5863-5866 [2] Tsuchiya K (1995), Model dynamics and function of a complex system (in Japanese). Control inf 39(1):29-34

[5] Y. Kanedal, N. Kamamichi, M. Yamakita1, K., Control of Linear Artificial Muscle Actuator Using IPMC, SICE Annual Conference in Fuhi, Fuhi tiniversiry, Japan, August 4-6.2003.

[6] K. Kim, J. Nam, Y. Tak, An Equivalent Circuit Model for Ionic Polymer-Metal Composites and Their Performance Improvement by a Clay-Based Polymer Nano-Composite Technique, J. Intelligent Material Systems and Structures, Vol.14, Octobr 2003.

[7] N.R. Tas, C. Gui, and M. Elwenspoek, Static Friction in Elastic Adhesive MEMS Contacts, Models and Experiment, IEEE, 2000. [2] Tsuchiya K (1995), Model dynamics and function of a complex system (in Japanese). Control inf 39(1):29-34

[8] K. Fuller, D. Tabor, The effect of surface roughness on the adhesion of elastic solids, Proc. R. Soc. Lond. A., vol. 345, pp.327-342.1975.

[9] Y. Rollot, S. Regnier and J. Guinot, Dynamical model for the micro-Manipulation by adhesion: experimental validations for determined conditions, Journal of Micromechatronics, Vol. 1,

[10] D. Sinan Haliyo, Yves Rollot and St´ephane R´egnier, Manipulation of micro-objects using adhesion forces and dynamical effects, IEEE, International Conference on Robotics and Automation, 2002. [2] Tsuchiya K (1995), Model dynamics and function of a complex system (in Japanese). Control inf 39(1):29-34

[11] D. S. Haliyo, S. Regnier, J. Guinot, [mü]MAD, the adhesion based dynamic micro-manipulator, European Journal of Mechanics A/Solids, 2003.

[12] P. Rougeot, S Regnier, N Chaillet1, Forces analysis for micro-Manipulation, International Symposium on Computational Intelligence in Robotics and Automation, IEEE, 2005.

[13] N. Tayebi Æ A. A. Polycarpou, Adhesion and contact modeling and experiments in microelectromechanical systems including roughness effects, Microsyst Technol, 2006.

[14] C. Canudas , H. Olsson, K. J. htrom, , and P. Lischinsky, "A New Model for Control of Micro-Systems with Friction," IEEE TRANSACTIONS ON AUTOMATIC CONTROL, VOL. 40, NO. 3, MARCH 1995.